STRESS PULSE LOADING OF A STATIONARY CRACK: EXPERIMENTAL AND NUMERICAL INVESTIGATION OF THE DISPLACEMENT FIELD

J. M. HUNTLEY[1] AND M. B. WHITWORTH[2]

1. Loughborough University, Department of Mechanical Engineering, Loughborough LE11 3TU, UK.

2. Campden & Chorleywood Food Research Association, Chipping Campden, GL55 6LD, UK.

ABSTRACT

This paper reports results of experimental and numerical studies of the interaction of a planar stress pulse with a stationary half-plane crack. The in-plane acceleration field resulting from a step pulse is integrated numerically to obtain displacement fields, which are presented as contour plots of the components parallel and perpendicular to the crack plane. Quasi-static eigenfunction expansions are fitted to the dynamic field to determine the accuracy with which they predict the true value of the stress intensity factor, as a function of the radius over which the fit is performed. For radii greater than about half of the dilatational wavefront radius, even fits to large numbers of parameters systematically overestimate the true value of K_I by up to 13%. Experimental results are presented from a through-crack in a plate of polymethyl methacrylate, with stress pulses generated by an electromagnetic loading device. Reasonable agreement is obtained between the optically measured stress intensity factor and that calculated from strain gauge records of the applied load history.

KEYWORDS

Dynamic fracture, stress wave loading, high speed photography, moiré fringes.

INTRODUCTION

One of the main aims of experimental studies of dynamic fracture is the measurement of the mode I dynamic stress intensity factor, K_{Id}. Many optical techniques have been developed to provide wholefield displacement or stress data; theoretical eigenfunction expansions of the relevant field are commonly fitted to these data and K_{Id} is assumed to be equal to the coefficient of the first term calculated from the fit. Photoelasticity fringe patterns have long been analysed in this way. More recently, the same approach has been taken with data from experimental techniques which measure in-plane displacements such as moiré interferometry (Arakawa *et al.*, 1991), moiré photography (Whitworth and Huntley, 1994; Whitworth, 1992), and speckle photography and interferometry (Huntley and Benckert, 1993).

Dynamic effects resulting from the steady motion of the crack tip through the material can be taken into account by fitting running-crack eigenfunctions. General expressions for stress and

displacement fields due to mode I, II and III cracks running at constant speed were derived by Nishioka and Atluri (1983). However, this approach may not be adequate under non-steady-state situations. A simple example is that of a stationary crack loaded by a stress pulse. The running crack tip eigenfunctions reduce to those for a quasi-statically loaded crack when the crack tip velocity is zero; the quasi-static fields are, however, inappropriate functions to use since each of the terms in a series expansion of the quasi-static stress or displacement field assumes the equations of equilibrium to be satisfied, which is clearly incorrect under conditions of stress wave loading. It seems likely therefore that there will be an error in the estimated value of K_{Id} resulting from this fitting procedure.

In the first half of this paper, the extent of the error is estimated for the particular case of a half-plane crack loaded by a planar stress pulse oriented parallel to the crack line and having a step time dependence. Eigenfunction expansions of the quasi-static displacement field are fitted to the calculated dynamic displacement field to determine the error in K_{Id}. In the second half of the paper, experimental results are presented from a stationary crack loaded dynamically, in which the displacement field is measured by sequences of high resolution moiré photographs recorded by a high speed camera. The error resulting from the fitting procedure can be estimated in this case from the stress intensity factor calculated from the applied load.

NUMERICAL EVALUATION OF THE DISPLACEMENT FIELD

The problem of the interaction of a step stress pulse with a half-plane crack (see Fig. 1) has been studied previously by, for example, Freund (1990), who derived the normal stress ahead of the crack tip and the form of the stress intensity factor. This analysis has subsequently been extended to include expressions for the in-plane acceleration field (Freund, 1991). The in-plane displacement field, $\boldsymbol{u} = (u_x, u_y)$, can then be calculated by a double integration of the accelerations with respect to time (Whitworth, 1992). Both the acceleration field analysis and details of the integration will be presented in a forthcoming publication.

Figure 2 shows contour plots of the displacement field components parallel and perpendicular to the crack line for the case Poisson's ratio $\nu = 0.499$ where the incident stress pulse and

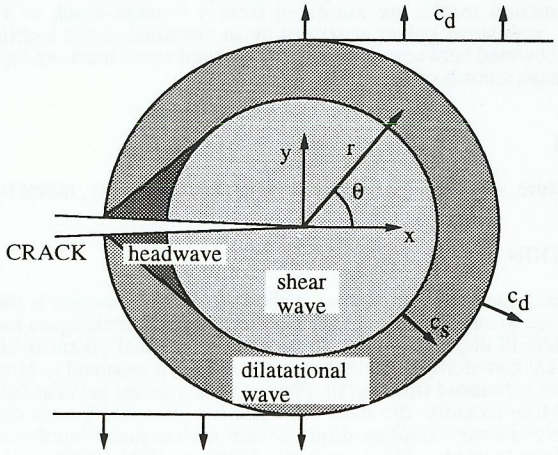

Fig. 1. Wavefronts produced by the interaction of a crack and a dilatational stress pulse. The dilatational and shear waves travel with speeds c_d and c_s respectively.

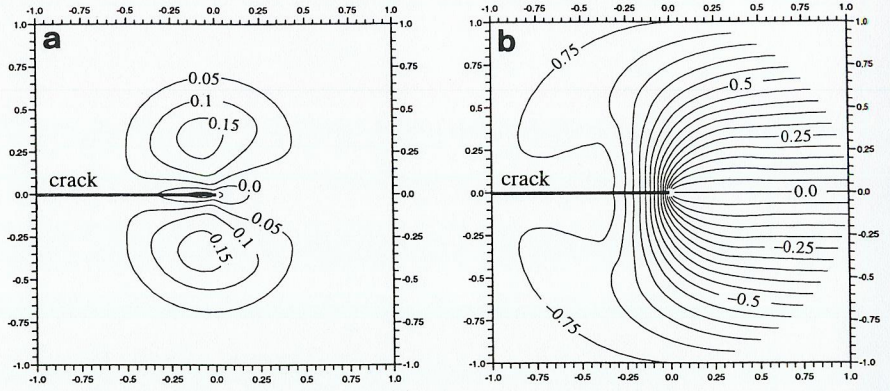

Fig. 2. Contour plots of the components of the displacement field parallel (a) and perpendicular (b) to the crack line under loading by a unit step pulse. Poisson's ratio = 0.499. Young's modulus has been taken as unity. Solutions for specific values of E, and for non-unit stress may be obtained by multiplying the displacements by a factor of σ/E.

Young's modulus are both taken to be unity. For generality, the results have been expressed in a dimensionless coordinate system, in which the dilatational wavefront has a radius of 1.0, and denoted by a subscript, n. The displacements have also been expressed in non-dimensional form, from which the true displacements may be calculated as

$$\boldsymbol{u} = \boldsymbol{u}_n \, t / a \qquad (1)$$

where t is the time after the arrival of the stress pulse at the crack line, and a is $1/c_d$ where c_d is the dilatational wave speed. The accuracy of the analysis was tested by examining the limiting behaviour of u_x and u_y at small distances, r, from the crack tip (Whitworth, 1992). As expected, both components were found to have the same $r^{1/2}$ dependence as for a crack under quasi-static mode I loading; furthermore the angular dependence was also found to be identical to that for the quasi-static mode I crack.

RESULTS OF FITTING QUASI-STATIC EIGENFUNCTION EXPANSION TO THE DYNAMIC FIELD

The quasi-static crack tip displacement field in a thin plate may be expanded as a series in half-integer powers of r, the distance from the crack tip (Barker *et al.*, 1985; Huntley and Field, 1988). The lowest order term varies as $r^{1/2}$, the coefficient of which is a linear combination of the mode I and mode II stress intensity factors, K_I and K_{II}. Close to the crack tip, the displacement field is three dimensional, but a two-dimensional solution is generally considered a sufficiently good approximation at radii greater than half the plate thickness (Yang and Freund, 1985). For a running crack under equilibrium conditions, the dynamic displacement eigenfunctions have been given by Nishioka and Atluri (1983). For the problem considered here, the crack is stationary; the x and y displacement components of the jth eigenfunction then reduce to the quasi-static solution:

$$\begin{pmatrix} u_x^{(j)} \\ u_y^{(j)} \end{pmatrix} = \frac{K_j^{\circ}\,(j+1)}{8\,\mu} \sqrt{\frac{r^j}{2\pi}} \begin{pmatrix} (2\kappa + j + 2(-1)^j)\cos(j\theta/2) - j\cos((2-j/2)\theta) \\ (2\kappa - j - 2(-1)^j)\sin(j\theta/2) - j\sin((2-j/2)\theta) \end{pmatrix}$$

$$+ \frac{K_j^*\,(j+1)}{8\,\mu}\sqrt{\frac{r^j}{2\pi}}\begin{pmatrix}(2\kappa + j - 2(-1)^j)\sin(j\theta/2) + j\sin((2-j/2)\theta)\\(-2\kappa + j - 2(-1)^j)\cos(j\theta/2) - j\cos((2-j/2)\theta)\end{pmatrix} \quad (2)$$

where μ is the shear modulus, and κ is equal to 3-4ν for plane strain, or $(3 - \nu)/(1 + \nu)$ for plane stress. The general displacement expression is a superposition of such eigenfunctions subject to appropriate boundary conditions. K_j^o and K_j^* are eigenvalues for symmetric (about the crack line) and asymmetric eigenfunctions respectively.

The stress intensity factor under plane stress for step pulse loading is given by Freund (1990) as:

$$K_{Id} = 2\sigma^*\sqrt{\frac{t(1-\nu^2)}{\pi a}} \quad (3)$$

where σ^* is the amplitude of the stress step. The availability of a solution for the displacement field under a particular example of dynamic conditions makes it possible to assess the error that can be expected in the value of the stress intensity factor when determined by such fitting methods, as a function of the number of eigenfunctions included in the fit. Although the errors may differ in detail for other forms of dynamic loading, examination of this particular solution exemplifies the magnitude of the errors than could typically be expected.

The first m symmetric eigenfunctions together with a rigid body displacement, were fitted to the y component of the calculated dynamic displacement field over a circular region of radius $r_n = r_{max}$, centred on the crack tip. The fit was performed over m symmetric eigenfunctions $(u_y^{(j)}(r,\theta)$ from Eqn. (2) with K_j^* set to zero) by minimising the sum,

$$S^2 = \sum_{i=1}^{N} W_i\left(u_y(r_i,\theta_i) - \delta - \sum_{j=1}^{m} u_y^{(j)}(r_i,\theta_i)\right)^2 \quad (4)$$

$u_y(r_i,\theta_i)$ are the dynamic displacements, δ is a rigid body displacement, and W_i is a weighting factor for the ith datapoint. There are therefore $n = m + 1$ variable parameters, these being δ and the m eigenvalues K_j^o. The fit was performed over a total of N calculated datapoints, spaced uniformly over 51 values of θ from $-\pi$ to $+\pi$, and for values of r_n spaced uniformly in increments of 0.025 from a minimum value of 0.025 to a chosen maximum value, r_{max}. The results of such fitting procedures depend on the spacing of the measured datapoints. In this case, the sampling of the data on a polar coordinate system provides a greater concentration of points towards the crack tip. Therefore, a weighting factor, W_i has been included in the fit. A value of $W_i = r_n$ was used in order to provide an equal weighting of points per unit area.

The value K_{Id}^{calc} of the stress intensity factor determined by the fitting procedure was calculated from the first eigenvalue as K_1^o. This has been compared with the true value of the dynamic stress intensity factor, calculated from Eqn. 3. The comparison of these values as a function of the number of parameters of the fit, and of the radius of the region of fitted data is shown in Fig. 3 for the case $\nu = 0.499$.

In all cases, the fit is poor for $n = 2$ and $n = 3$, and significantly underestimates the true value of the stress intensity factor. In general, for higher numbers of parameters, the stress intensity factor is overestimated. The deviation of the eigenfunction expansion from the dynamic solution increases with increasing radius, similarly affecting the accuracy of the determination of the stress intensity factor. For $n = 4$ to 7, the deviation from the true value increases above approximately $r_{max} = 0.3$, whereas for $n = 8$ to 10, the accuracy improves significantly, deteriorating only above about $r_{max} = 0.6$. In general, the deviation in K_{Id}^{calc} is greater, and occurs at lower values of r_{max} for larger values of Poisson's ratio.

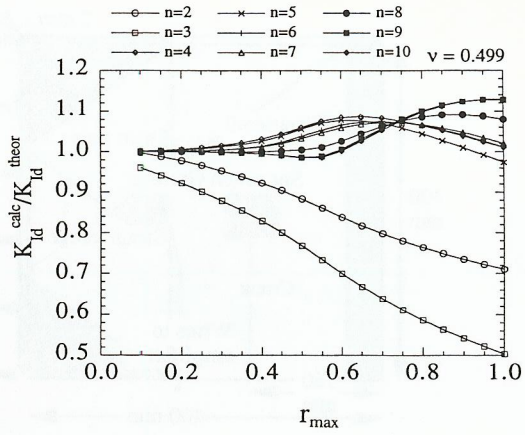

Fig. 3. Stress intensity factor K_{Id}^{calc} normalised by theoretical value, K_{Id}^{theor} as a function of maximum radius, r_{max}, over which the least squares fit is carried out. Poisson's ratio = 0.499.

EXPERIMENTAL

Experiments have been carried out involving a similar loading arrangement to that analysed theoretically in the previous sections. An electromagnetic pulse generator loads a notch with a tensile stress wave; a strain gauge record of the incoming stress wave is used to compute the applied stress intensity factor, and this is compared with the results of fitting an eigenfunction expansion to the measured displacement field. The technique used to measure the displacements was high resolution moiré photography (Whitworth and Huntley, 1994), in which high frequency phase gratings are applied to the specimen and imaged with a specially modified camera lens onto a stationary reference grating. The effective grating frequency is 150 lines mm^{-1} giving a basic sensitivity of 6.7 μm fringe^{-1}.

Figure 4 illustrates the specimen geometry, consisting of a rectangular polymethyl methacrylate (PMMA) plate containing a long crack. Loading is provided by a stress pulse generator consisting of a coil of wires bonded to the right hand edge of the plate; a 10-stage capacitor-inductor network is discharged through the coil using a spark gap as a triggering device. The current pulse of ~2 kA provides an approximately square load pulse of ~1.6 kN lasting around 100 μs (Whitworth, 1992). The resulting dilatational pulse propagates through the plate, and is trailed by shear waves which initiate at the plate edges as the pulse passes.

Figure 5 shows a single frame from one sequence of high resolution moiré fringe patterns recorded by a high speed camera (Imacon 790) over a 25 mm × 25 mm field of view centered on the crack tip. The crack is vertical with its tip in the centre of the field of view. The grating was vertical so the fringe represents the displacement component perpendicular to the crack line (u_y in the coordinate system of Fig. 1). Figure 6 is a set of contour maps showing u_y calculated from the sequence of images. The magnitude of the strain field (proportional to the contour density) can be seen to increase with time from the initial application of the dynamic load. Frame 1 was recorded 10.5 μs after the arrival of the stress wave at the crack line.

The eigenfunctions (Eqn. 2) were fitted to the measured displacements by minimising the function given by Eqn. 4. In addition to δ, a term $\Omega r_i \cos\theta_i$ was included to allow for the possibility of rigid body rotation. The weights W_i were set to unity since the data were obtained

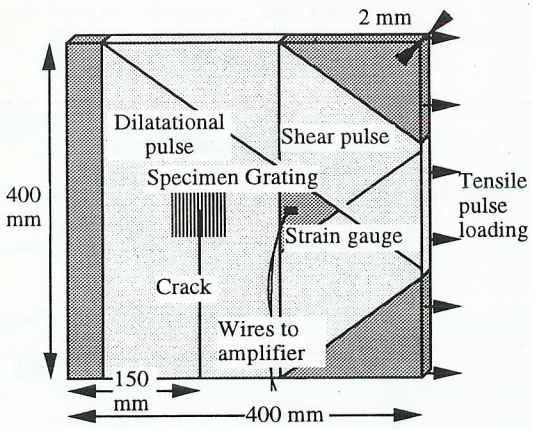

Fig. 4. PMMA plate specimen used for dynamic fracture experiments. A tensile load is applied to the entire right hand edge of the plate for a duration of about 100 μs, generating a dilatational pulse. As this traverses the plate, it initiates shear pulses at the top and bottom plate edges. The dilatational pulse is incident on a vertical crack at the tip of which a moiré specimen grating is mounted, allowing the displacement field to be measured.

Fig. 5. Single fringe pattern from a high speed sequence recorded at the tip of a crack in a PMMA plate. The field of view is 25 mm × 25 mm, and the inter-frame time is 5 μs.

on a square mesh. Elastic constants E = 5.562 GPa and ν = 0.34 were used in the fit; these are appropriate values for PMMA at loading times of 10^{-5} - 10^{-6} s (Read and Dean, 1978).

Figure 7 shows the stress intensity factors calculated from 7-parameter (m = 5) fits to each of the displacement fields shown in Fig. 6, together with values calculated from two further loadings of the plate, at later times after arrival of the pulse. The solid line shows a prediction obtained by convolving a strain gauge record of the input stress profile with the theoretical

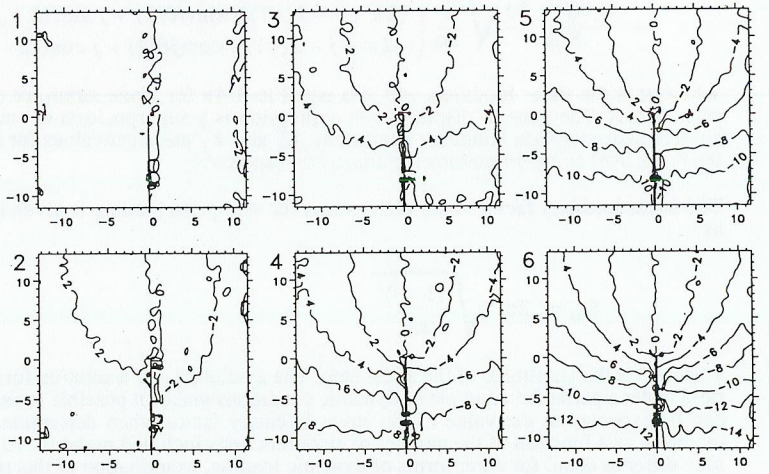

Fig. 6. Contour plots of horizontal in-plane displacement component obtained from high speed sequence (Fig. 5 corresponds to frame 6). Dimensions are in mm; contour heights are in μm.

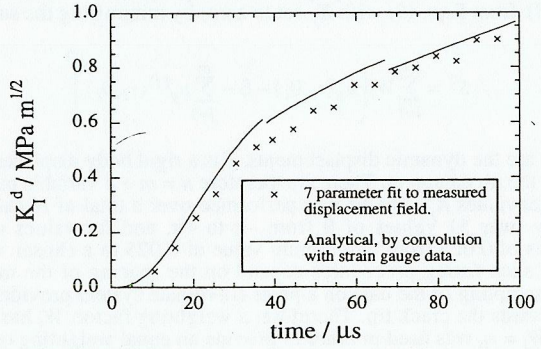

Fig. 7. Dynamic mode I stress intensity factor, K_{Id} as a function of time. The points result from a 7-parameter eigenfunction fit to measured displacement fields. The line is the result of convolving a theoretical step pulse solution with a strain gauge trace of the input stress profile.

solution for step pulse loading of an elastic plate under plane stress conditions, given by Eqn. 3. The predicted and measured K values are in agreement to within 5 to 10%. For $t \geq 15$ μs, r_{max} is less than one third of the radius of the expanding dilataional wave, and the results from the previous sections therefore indicate that a sufficient fit should be provided by the seven (m = 5) parameter fit. A possible explanation for the remaining discrepancy is a systematic misidentification of the crack tip position on the experimentally measured fields. An error of about 0.2 mm (2 pixels) parallel to the crack line is sufficient to explain the observed discrepancy, and is made plausible by the increased error at earlier times when the fringes are straighter and the crack tip is harder to locate.

CONCLUSIONS

The in-plane displacement field around a stationary crack following loading by a planar step stress pulse has been calculated numerically from an analytical solution for the acceleration field. The results obtained were found, as expected, to be in good agreement with the quasi-static solution very close to the crack tip. When eigenfunction expansions of the quasi-static displacements were fitted to the calculated dynamic displacement fields, significant errors in K_I were found as the radius of fitting approached the radius of the diffracted dilatational wave. The maximum radius of fitted data for which satisfactory determinations of K_I can be obtained by this procedure increases with the number of eigenfunctions included in the fit. However, even fits with large numbers of parameters can in the worst case systematically overestimate the true value of K_I by up to 13%. Experiments have also been carried out to test the reliability of estimating K_I in this way. In this case the results of the fitting were compared with K values calculated from strain gauge records of the incoming stress pulse. Agreement of results to within the experimental error of 5-10% was obtained.

ACKNOWLEDGMENTS

The authors are grateful to Prof. L. B. Freund for supplying the theoretical solution for the acceleration field and for many useful discussions. J.M.H. was supported by a Research Fellowship from the Royal Society; M.B.W. by a studentship from the Science and Engineering Research Council (SERC) and from Nuclear Electric Plc.

REFERENCES

Arakawa, K., Drinnon, R. H., Kosai M. and Kobayashi, A. S. (1991) Dynamic fracture-analysis by moiré interferometry. *Exp. Mech.* **31**, 306-309.

Barker, D. B., Sanford, R. J. and Chona, R. (1985) Determining K and related stress-field parameters from displacement fields. *Exp. Mech.* **25**, 399-407.

Freund, L. B. (1990) *Dynamic Fracture Mechanics*. Cambridge University Press, Cambridge.

Freund, L. B. (1991) Private communication.

Huntley, J. M. and Benckert, L. (1993) Measurement of dynamic crack tip displacement field by speckle photography and interferometry. *Opt. Lasers Eng.* **19**, 299-312.

Huntley, J. M. and Field, J. E. (1988) Measurement of crack tip displacement field using laser speckle photography. *Eng. Fract. Mech.* **30**, 779-790.

Nishioka, T. and Atluri, S. N. (1983) Path-independent integrals, energy release rates, and general solutions of near-tip fields in mixed-mode dynamic fracture mechanics. *Eng. Fracture Mech.* **18**, 1-22.

Read, B. E. and Dean, G. D. (1978) The determination of dynamic properties of polymers and Composites. Adam Hilger, Bristol, U.K..

Yang, W. and Freund, L. B. (1985). Transverse shear effects for through-cracks in an elastic plate. *Int. J. Solids Struct.* **21**, 977-994.

Whitworth, M. B. (1992) Application of high resolution moiré photography to dynamic fracture studies. PhD thesis, University of Cambridge.

Whitworth, M. B. and Huntley, J. M. (1994). Dynamic stress analysis by high resolution reflection moiré photography. *Opt. Eng.* **33**, 924-931.